



Community metabolism, phytoplankton size structure and heterotrophic prokaryote production in a highly productive upwelling zone off northern Chile

Barbara Jacob^{1,2,3,*}, Giovanni Daneri^{3,4}, Renato A Quiñones^{3,5}, Marcus Sobarzo⁵

¹Programa de Postgrado en Oceanografía, Departamento de Oceanografía, Universidad de Concepción, Casilla 160-C, Concepción, Chile

²Centro de Ciencias y Ecología Aplicada (CEA), Universidad del Mar, Carmen 446, Cerro Placeres, Valparaíso, Chile

³Centro de Investigación Oceanográfica en el Pacífico Sur-Oriental (COPAS), Universidad de Concepción, Casilla 160-C, Concepción, Chile

⁴Centro de Investigación en Ecosistemas de la Patagonia (CIEP), Bilbao 449, Coyhaique, Chile

⁵Departamento de Oceanografía, Universidad de Concepción, Casilla 160-C, Concepción, Chile

ABSTRACT: We investigated the ecological factors affecting net ecosystem metabolism (as the ratio of gross primary production to community respiration) by studying functional relationships between total and fractionated autotrophic biomass, heterotrophic prokaryote production, nutrients and net ecosystem metabolism, considering short-term (daily) and seasonal scales of variability in oceanographic conditions and wind stress. These studies were performed at 2 coastal upwelling sites off northern Chile (Chipana, ~21° S; Mejillones, ~23° S) in winter 2005, summer 2006, winter 2006 and summer 2007. Changes in the direction and persistence of the upwelling, which is driven by wind stress on a synoptic scale (6 d), appeared to be an important factor modulating phytoplankton size structure. Gross primary production did not show seasonality, probably because of the permanent equatorward wind regime off northern Chile. The phytoplankton community was dominated by the microphytoplankton size fraction (>20 µm), which was largely responsible for the variability of the total phytoplankton biomass. We found that the increase in contribution of large phytoplankton cells could generate net autotrophy in response to increased nitrate concentrations in the mixed layer, emphasizing that the degree of decoupling between gross primary production and community respiration may be primarily controlled by upwelling. Our results showed that the degree of coupling between heterotrophic prokaryote production and gross primary production as well as the amount of organic matter processed by prokaryotes vary with changes in the dominance of autotrophic and heterotrophic processes in the microplanktonic community.

KEY WORDS: Phytoplankton size structure · Net ecosystem metabolism · Prokaryote net production · Upwelling system · Humboldt Current System

Resale or republication not permitted without written consent of the publisher

INTRODUCTION

The rationale for ecological models of carbon transfer in pelagic food webs that support high fish landings is based on the idea that large phytoplankton can be transferred to fish through an efficient herbivorous food web (Steele 1974). Nevertheless, empirical evidence has demonstrated that prokaryotes and their micro-

protozoan predators account for a large fraction of the ocean metabolism and represent an alternative pathway for carbon and energy other than the classical food chain (Pomeroy 1974, Sieburth et al. 1978, Williams 1981, Azam et al. 1983, Jahnke & Craven 1995).

The Humboldt Current System (HCS) off Chile is one of the most productive ecosystems of the world (Montecino et al. 2006), with primary production rates

of up to $25.8 \text{ g C m}^{-2} \text{ d}^{-1}$ (Montero et al. 2007) and high fish landings (Leal et al. 2010). Several studies carried out in the main upwelling centers off Chile have attempted to unravel how carbon flows through the food web are affected by the heterotrophic prokaryote community. Simple correlations between gross primary production (GPP) and bacterial secondary production suggest that bacterioplankton consume the bulk of marine organic matter produced by photosynthesis in the photic zone of the HCS (Troncoso et al. 2003, Montero et al. 2007). Studies based on the structure of the planktonic food web and carbon dynamics support this view, showing that the microheterotrophic pathway could be an important carbon link in upwelling ecosystems (Cuevas et al. 2004, Vargas et al. 2007, Quiñones et al. 2010). Therefore, it is crucial to allocate more efforts towards reassessing the ecological role of the phytoplankton community and heterotrophic prokaryote production in biogeochemical fluxes and the transfer of energy and matter in major upwelling systems such as the HCS.

The capacity of the ecosystem to export organic matter can be estimated by the degree of imbalance between GPP and community respiration (CR). The GPP:CR ratio is a useful index of the trophic condition of aquatic ecosystems; operationally, this ratio has been defined as net ecosystem metabolism (Smith & Hollibaugh 1997). If GPP:CR is >1 , the ecosystem is net autotrophic, whereas if GPP:CR is <1 , the ecosystem is net heterotrophic. The balance between net autotrophy and net heterotrophy within aquatic systems may be strongly affected by changes in the phytoplankton size structure (Smith & Kemp 2001, Teira et al. 2001) as well as by the nature of exogenous inputs (Nixon & Pilson 1984, Kemp et al. 1997, Smith & Hollibaugh 1997). Typically, when $\text{GPP} > \text{CR}$, surplus organic matter can be exported to either higher trophic levels or to other areas (Quiñones & Platt 1991). In contrast, when $\text{GPP} < \text{CR}$, that system must, at least partially, rely on allochthonous carbon subsidies (Duarte & Agustí 1998).

Knowledge about the ecological factors controlling the ecosystem metabolism in the HCS is scarce. In highly productive ecosystems such as central-southern Chile (36° S), the imbalance between GPP and CR may respond to variations in nutrient concentrations induced by the intensification of wind-driven upwelling in austral spring and summer (Montero et al. 2007). The latter authors also suggest that the dominance of nano- and picophytoplankton cells during non-productive seasons (Böttjer & Morales 2005) may be responsible for the GPP:CR ratio of <1 . Because the phytoplankton size structure has been identified as the principal mechanism controlling the cycling of carbon through the pelagic ecosystem (Legendre & Le Fèvre 1989, Legendre et al. 1993, Tremblay & Legendre 1994,

Legendre & Rassoulzadegan 1995, Nielsen & Hansen 1995, Kiørboe 1996, Legendre & Michaud 1998, Tami-gneaux et al. 1999), changes in the size structure of the autotrophic community should determine changes in the GPP:CR ratio.

In northern Chile, upwelling intensity fluctuates because wind stress is variable, especially on daily to weekly scales (Escribano et al. 2004a), producing short-term variability (3–5 d) of both the nanoplankton and microplankton community composition (Aguilera et al. 2009). The latter authors indicate that an entire community can be modified in terms of species composition and size structure over the course of a few days. In addition, the HCS is affected by both intra-seasonal (McPhaden 2008) and interannual atmospheric forcing (Escribano et al. 2004b) due to the El Niño Southern Oscillation (ENSO), which has a considerable effect on the temperature, oxygenation and stratification of the water column and the upwelling regime (Aguilera et al. 2009). Here, we assessed the ecological factors affecting the net ecosystem metabolism by studying functional relationships between phytoplankton size structure, heterotrophic prokaryote production, nutrients and net ecosystem metabolism considering short-term (daily) and seasonal-scale changes in oceanographic conditions and wind stress at 2 coastal upwelling sites off northern Chile: Chipana and Mejillones. Our goal was to establish whether the GPP:CR ratio varied as a function of nitrate and chlorophyll *a* (chl *a*) concentrations in the mixed layer, both of which are related to upwelling dynamics. We hypothesized that greater nutrient availability in the mixed layer increases the contribution of large phytoplankton cells, which, in turn, increases the GPP:CR ratio. In addition, we assessed the role of heterotrophic prokaryote activity related to changes in the GPP:CR ratio.

MATERIALS AND METHODS

Study area. The coastal ocean in northern Chile is characterized by intermittent wind-driven upwelling events (Blanco et al. 2001) and high spatial and temporal variability in primary production (0.1 to $9 \text{ g C m}^{-2} \text{ d}^{-1}$; Daneri et al. 2000). The microbial realm, especially heterotrophic prokaryotes, has been shown to be a key component of the carbon cycling in this upwelling area (Troncoso et al. 2003). The value reported by these same authors for bacterial secondary production (ca. $5000 \text{ mg m}^{-2} \text{ d}^{-1}$) measured in the coastal area of Antofagasta is one of the highest in the literature. In turn, a significant proportion of primary production may be utilized by bacteria (ca. 63 to 97%) (Troncoso et al. 2003), which suggests that bacteria are capable of pro-

cessing an important fraction of the organic carbon fixed by algal activity in this northern region. This area also exhibits a permanent oxygen minimum zone (Ulloa & Pantoja 2009) that is largely associated with high organic production and O_2 consumption through the heterotrophic utilization of organic matter.

The area off northern Chile is subjected to strong interannual variability due to ENSO (Escribano et al. 2004b). Changes in water column conditions during warm episodes have drastic effects on biological production rates (Barber et al. 1996). Thus, oceanographic anomalies associated with the intrusion of warmer oligotrophic waters to the coast reduce the upwelling of cold, nutrient-rich waters in the upper 100 m. An oligotrophic regime appears to result in a higher dominance of pico- and nanophytoplankton in inshore areas and, consequently, low primary production (Iriarte & González 2004) and community respiration rates (Eissler & Quiñones 1999).

Sampling. The 2 study areas were located in northern Chile, at Chipana ($21^{\circ}19'S$, $70^{\circ}05'W$) and Mejillones Bay ($23^{\circ}00'S$, $70^{\circ}27'W$), 4.8 and 3.2 km, respectively, from the coast on the continental shelf (Fig. 1). Sampling was conducted at a fixed station anchored on the continental shelf (90 m) in each area. Seawater was collected for physical-chemical parameters, *in situ* experiments and standing stocks of microbial assemblages. At Chipana, sampling was carried out in winter 2005 (22 to 26 July), summer 2006 (4 to 8 February), winter 2006 (1 to 8 July) and summer 2007 (1 to 8 February); at Mejillones, sampling was done in summer 2006 (24 to 28 January). Vertical profiles of temperature, salinity, oxygen and photosynthetically active radiation (PAR) were obtained with a Seabird SBE-19 CTD every 24 h. Water samples were collected with 10 l Niskin bottles at 5, 10, 20, 50 and 85 m every 48 h and from depths of 5, 10 and 20 m daily. All collected samples were used to determine dissolved oxygen and inorganic nutrient concentrations, and total and fractionated chl *a* biomass (<2 μm , 2–20 μm and >20 μm). Samples taken every 48 h were used to determine the metabolic rates of the microplankton community.

Physical forcing. To characterize seasonal changes in winds and the physical environment, we used CTD vertical profiles (Chipana and Mejillones) and wind speed and direction data (only for Chipana) obtained from meteorological stations at Diego Aracena airport in Iquique ($20^{\circ}32'S$, $70^{\circ}11'W$; 52 m elevation). Hourly records of coastal winds for the seasonal sampling in Chipana were processed to calculate the daily cumulated wind stress, considering 11 d for each sampling period. Wind stress (τ) was calculated as:

$$\tau = \rho_a C_D |\vec{V}| \vec{V} \quad (1)$$

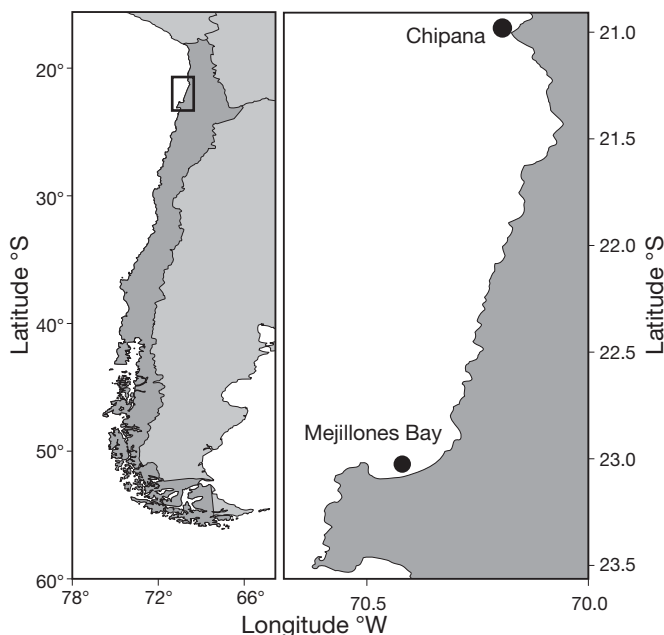


Fig. 1. Location of sampling sites in the northern coastal upwelling region off Chile in the eastern South Pacific, showing Chipana ($21^{\circ}19'S$, $70^{\circ}05'W$) and Mejillones Bay ($23^{\circ}00'S$, $70^{\circ}27'W$). Measurements of hydrographical parameters, *in situ* incubations of metabolic processes and determinations of standing stocks of biomass were performed at the indicated fixed stations. Four oceanographic cruises at Chipana, 1 at Mejillones

where ρ_a is air density (kg m^{-3}), C_D is the drag coefficient and \vec{V} is wind velocity (m s^{-1}).

Inorganic nutrients and total and fractionated chl *a*. Samples to determine nitrate, nitrite, phosphate and silicic acid were obtained daily from 5, 10 and 20 m. These samples were filtered (GF/F) and frozen (-20°C) until analysis in the laboratory. Nitrate and phosphate were determined spectrophotometrically as in Strickland & Parsons (1968). Nitrite was analyzed using an automated nutrient analyzer (ALPKEM, Flow Solution IV) following the protocol of the US Environmental Protection Agency (Office of Research and Development Environmental Monitoring and Support Laboratory, Cincinnati, OH; Method 353.2).

Size-fractionated chl *a* (pico-, nano- and microplankton size fractions) was measured at the same depths used to obtain samples for inorganic nutrients. Seawater samples were filtered and fractionated following these steps: (1) for the nanoplankton fraction (2 to 20 μm), seawater (200 ml) samples were pre-filtered at 20 μm pore size and collected on a 1.7 μm filter (GF/A); (2) for the picoplankton fraction (0.7 to 2 μm), seawater (200 ml) was pre-filtered at 1.7 μm and collected on a 0.7 μm filter (GF/F); and (3) for the whole phytoplankton community, seawater (200 ml) was filtered through 0.7 μm . The chl *a* content of the micro-phytoplankton

fraction was obtained by subtracting the nano- and picoplankton fractions from the whole phytoplankton chl *a* biomass.

GPP and CR experiments. *In situ* incubations for GPP and CR estimates were undertaken during the 5 oceanographic cruises. A total of 16 experiments were conducted with water samples obtained from within the mixed layer (5, 10 and 20 m at Chipana; 5, 10 and 15 m at Mejillones) and within the euphotic zone. The bottom boundary of the euphotic zone was determined as the depth at which PAR fell to 1% of the surface values using a Secchi disk. GPP and CR measurements were estimated from changes observed in dissolved oxygen concentrations after incubating *in situ* light and dark bottles (Strickland 1960). Water from Niskin bottles was transferred to 125 ml borosilicate bottles (gravimetrically calibrated). At each incubation depth, 5 bottles were immediately treated with the Winkler reagents and used to determine the initial oxygen concentration, and another 5 light and dark bottles were used to determine the final oxygen concentration. Clear and darkened bottles (light and dark) were incubated *in situ* for 24 h, attached to a surface buoy mooring anchored to the ocean floor (~90 m).

Dissolved oxygen concentrations were determined manually according to the Winkler method (Strickland & Parsons 1968) using an automatic Dosimat Metrohm 665 burette and by visual end-point detection. The average coefficient of variation for replicate samples was 0.4%. GPP values were converted from oxygen to carbon units using a conservative photosynthetic quotient (PQ) of 1.4 (i.e. characteristic of systems with high new production; Laws 1991) for periods with high nitrate levels (e.g. July 2005, January 2006 and February 2007) and maintaining a PQ of 1.25 (e.g. characteristic of systems in which regenerated production could be important) for periods of low nutrients (e.g. February and July 2006). For CR estimates, a respiratory quotient (RQ) of 1 was used. Rates of GPP and CR were calculated as follows: GPP = mean $[O_2]$ in 24 h light – mean $[O_2]$ dark bottles; CR = mean initial $[O_2]$ – mean $[O_2]$ in 24 h dark bottles. Discrete GPP and CR rates were integrated for the whole mixed layer using a polynomial fit. Seasonal differences in total integrated GPP and CR were determined by a non-parametric Mann-Whitney *U*-test.

Operationally, we use the term 'coupling' when most of the photosynthetic organic matter production is consumed within a 24 h cycle (i.e. GPP = CR). 'Decoupling' is used when GPP and CR occur temporally out of phase for more than 24 h and, therefore, GPP:CR is >1 or <1. The 24 h time scale was chosen because it corresponds to the incubation time used in our primary production and respiration *in situ* experiments.

Prokaryote net production. In pelagic ecosystems, bacteria coexist with archaea (Karner et al. 2001, Herndl et al. 2005), and both consume leucine. Although some studies have argued that archaea are not abundant in the surface layer of most oceanic regimes (Robinson 2008), the archaeal abundance in the first 60 m of the northern portion of the HCS off Chile constitutes between 10 and 50% of the prokaryote rRNA (Quiñones et al. 2009). Therefore, herein, the term 'prokaryote net production' (PNP) includes both bacterial and archaeal production. PNP experiments were carried out using the deep samples obtained for *in situ* GPP and CR experiments during the 5 oceanographic cruises. PNP was estimated by incorporating L- $[^{14}C(U)]$ -leucine (300 mCi mmol⁻¹, 50 nM final concentration) into proteins (Simon & Azam 1989). Three 10 ml samples from each sampling depth were incubated under illuminated conditions, and one sample was kept in the dark. Samples were incubated for 1 h and then poisoned with 0.2 µm filtered and buffered formaldehyde. All incubations were stopped by adding cold analytical grade trichloroacetic acid (50% w/v). After 10 min, the tube contents were filtered (0.22 µm pore size, GSWP Millipore). Dried filters were transferred to borosilicate scintillation vials and kept cold until radio-isotopic analysis. In the laboratory, analytical grade ethyl acetate and 10 ml liquid scintillate Eco-lite (+) (ICN) were added to the vials. All samples were measured in disintegrations per minute (dpm) using a Packard 1600 TR liquid scintillation counter. The transformation of the incorporation rates of leucine into prokaryote carbon followed the rationale of Simon & Azam (1989).

RESULTS

Oceanographic setting

Sea surface temperatures differed by approximately 4°C between austral winter (July 2005) and summer (February 2006) for both study areas. Vertical profiles of temperature and oxygen exhibited slight daily differences, as shown for the Chipana sampling site (Fig. 2). On a seasonal scale, the mixed layer was deeper in winter and the water column was stratified in summer. These vertical profiles (Fig. 2) also showed a mixed layer in the top 20 m, coinciding with the depth of the oxygen minimum zone (1 ml l⁻¹) at both sampling sites. In summer, irradiance ranged from 359 to 1180 E at the surface and decayed exponentially to 1% PAR between 10 and 20 m depth. However, in winter, irradiance ranged from 280 to 1720 E at the surface, falling to 1% PAR at 10 m depth (data not shown). The highest southerly cumulative wind stress

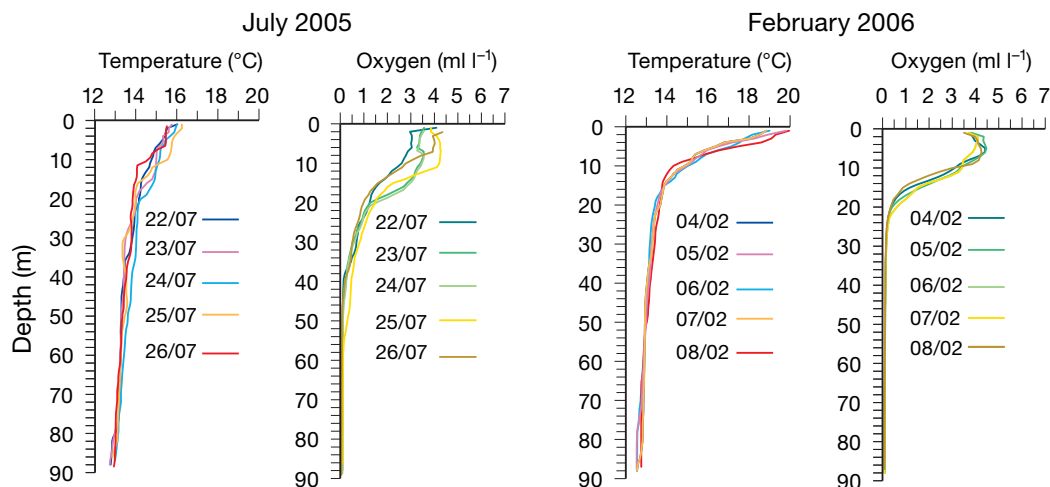


Fig. 2. Representative vertical depth profiles of temperature and oxygen concentrations in winter (July 2005) and summer (February 2006) at Chipana. Dates are dd/mm

(favourable to upwelling) occurred in February 2006 ($9 \text{ N m}^{-2} \text{ d}^{-1}$) (Fig. 3), whereas intermediate values ($5 \text{ N m}^{-2} \text{ d}^{-1}$) were observed in July 2005 and February 2007 (Fig. 3). During winter 2005, January 2006, and February 2006 and 2007, the water column at Chipana and Mejillones Bay presented cold conditions characterized by a very shallow 15°C isotherm and oxycline (Fig. 4c). In July 2006, the wind stress direction was clearly not favourable to upwelling (i.e. 2, 4 and 6 July 2006; Fig. 5), with conditions of minimum daily cumulative wind stress ($2 \text{ N m}^{-2} \text{ d}^{-1}$; Fig. 3). The change in wind pattern that took place in July 2006 promoted a sharp deepening of the 15°C isotherm and oxygen minimum zone ($<1 \text{ ml l}^{-1}$) to 35 and 50 m, respectively (Fig. 4c).

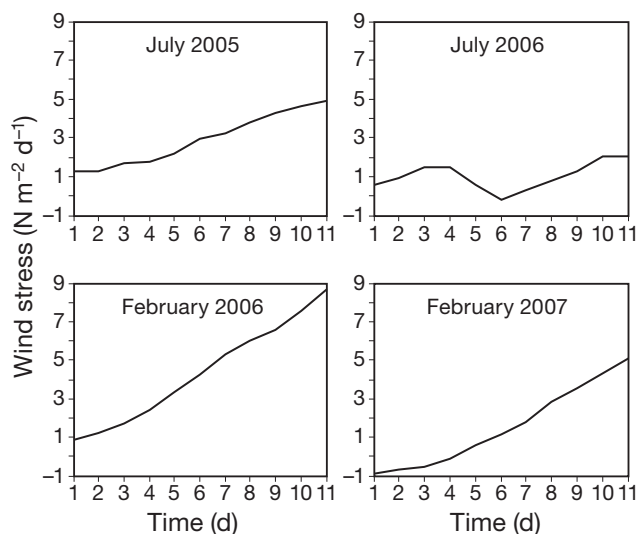


Fig. 3. Accumulated wind stress, Chipana

Total and size-fractionated chl *a* and nutrients

The highest chl *a* concentrations, integrated for the mixed layer (20 m), were found in July 2005 (mean = 214.6 mg m^{-2}) and February 2007 (mean = 256.5 mg m^{-2}), and the lowest in January 2006 (mean = 81.8 mg m^{-2}), February 2006 (mean = 46.3 mg m^{-2}) and July 2006 (mean = 68.4 mg m^{-2}) (Table 1). The relationship between total chl *a* and size-fractionated biomass (as discrete values) showed that microphytoplankton ($>20 \mu\text{m}$ size fraction) was largely responsible for the variability of the total phytoplankton biomass ($r^2 = 0.99$, $n = 39$, $p < 0.0001$, $y = -0.75 + 0.98x$), whereas nanophytoplankton (2 to $20 \mu\text{m}$ size fraction) and picophytoplankton ($<2 \mu\text{m}$ size fraction) remained at relatively constant background levels, not contributing to the increase of total standing stocks (Fig. 6a).

The relationships between percentage contribution of size-fractionated chl *a* and total chl *a* biomass (as discrete values) in the top 20 m of the mixed layer indicated that cells $>20 \mu\text{m}$ contributed as much as 80 to 98% when the total chl *a* was $>15 \mu\text{g chl a l}^{-1}$ (Fig. 6b). In contrast, the highest contribution (20 to 70%) of small cells ($<2 \mu\text{m}$, 2 – $20 \mu\text{m}$) occurred at total chl *a* biomass values below $15 \mu\text{g chl a l}^{-1}$ (Fig. 6b). Cells $<2 \mu\text{m}$ represented $<5\%$ of the total chl *a* (Fig. 6b). The depth-integrated values of size-fractionated chl *a* (0 to 20 m) showed that, in July 2006, picophytoplankton accounted for 34% of total chl *a* (Table 1). The comparison of nutrient concentrations in the mixed layer (0 to 20 m) between seasons indicated that the highest concentrations occurred in July 2005, January 2006 and February 2007, and the lowest in February 2006 and July 2006 (Fig. 4a,b). Integrated total chl *a* was significantly correlated with NO_3^- ($r = 0.85$, $p < 0.05$, $n = 13$), PO_4^{3-} ($r = 0.84$, $p < 0.05$, $n = 13$) and Si ($r = 0.8$, $p < 0.05$, $n = 13$).

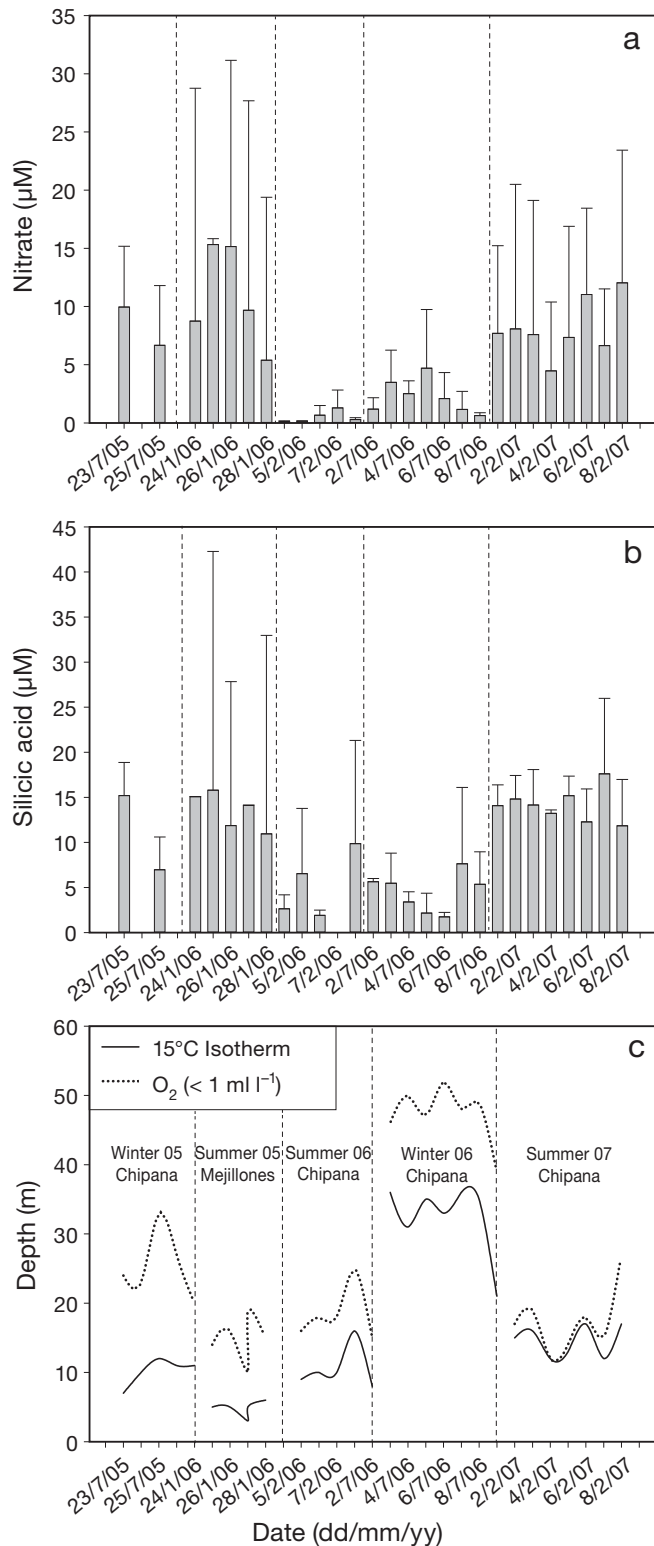


Fig. 4. Daily and seasonal variability of average concentrations of (a) nitrate and (b) silicic acid in the top 20 m of the water column, and (c) the depth of the 15°C isotherm and O_2 concentration $< 1 \text{ ml l}^{-1}$ in July 2005, January 2006, February 2006, July 2006 and February 2007 in Chipana and Mejillones. Data are from the CENSOR cruise in northern Chile

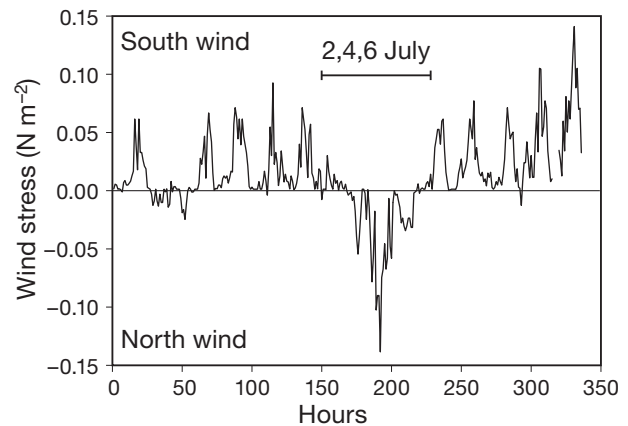


Fig. 5. Wind stress time-series for July 2006, obtained from the meteorological station at Diego Aracena airport in Iquique, concurrent with the CENSOR cruise at Chipana

GPP, CR and the GPP:CR ratio

Unlike chl *a* biomass, depth-integrated GPP and CR in the mixed layer did not show significant seasonal differences ($U = 17.5$, $p > 0.05$, $n = 7$; $U = 11$, $p > 0.05$, $n = 7$, respectively). Primary production peaked in July 2005 ($10.4 \text{ g C m}^{-2} \text{ d}^{-1}$) and February 2007 ($8.6 \text{ g C m}^{-2} \text{ d}^{-1}$) (Table 2), coincident with the highest mean concentrations of nitrate ($8.3 \mu\text{M}$) and silicic acid ($14.2 \mu\text{M}$) in the mixed layer. The GPP:CR ratio was used to determine the net ecosystem metabolism of the microplanktonic community. Operationally, and according to our experimental protocol, we defined the microplankton community as those organisms $< 200 \mu\text{m}$; thus, CR includes the respiration of all organisms within this size range in the water sample. If the ratio is > 1 , the ecosystem is considered to be net autotrophic, whereas a ratio of < 1 indicates that the ecosystem is net heterotrophic. During net autotrophy, surplus organic matter is typically available to be exported either to higher trophic levels or to adjacent areas (by physical transport) or the deeper ocean (Quiñones & Platt 1991). During net heterotrophy, the system requires allochthonous organic matter to sustain the metabolic demand of the microplanktonic community. We found that the microbial community inhabiting the mixed layer in the coastal system off Chipana is able to shift from one trophic state to another within a week (7 to 8 d), as observed at this study site in July 2006 (GPP:CR ratio = 0.8 to 2.19) and February 2007 (GPP:CR ratio = 0.2 to 2.7) (Table 2). The correlation between average nitrate within the mixed layer and the depth-integrated GPP:CR ratio was high ($r = 0.93$, $n = 11$, $p < 0.05$) (Fig. 7a), indicating that the GPP:CR ratio increased linearly along with increments in the nitrate concentration of the mixed layer. In turn, the correlation between depth-integrated (mixed

Table 1. Summary of mixed-layer integrated total chlorophyll *a* (chl *a*) values and the percentage contribution made by 3 chl *a* size fractions: picophytoplankton (<2 μm), nanophytoplankton (2 to 20 μm) and microphytoplankton (>20 μm). Data are from the CENSOR cruise in Chipana (21° S) and Mejillones (23° S), northern Chile

Area	Date (dd/mm/yy)	Chl <i>a</i> (mg m ⁻²)	Chl <i>a</i> (%)		
			<2 μm	2–20 μm	>20 μm
Chipana	23/07/05	238.61	–	–	–
	25/07/05	190.53	–	–	–
Mejillones	24/01/06	95.25	–	–	–
	26/01/06	66.15	3	38	59
	28/01/06	84.19	2	40	58
Chipana	04/02/06	35.24	–	40	–
	06/02/06	64.51	10	80	10
	08/02/06	39.42	5	50	45
	02/07/06	44.32	8	64	28
	04/07/06	40.52	2	55	43
	06/07/06	33.35	4	52	44
	08/07/06	153.87	34	2	65
	02/02/07	184.03	0.7	6	93
	04/02/07	321.47	1.7	4.7	94
	06/02/07	314.31	1.9	4.6	94
	08/02/07	206.26	1.2	10.5	86

layer) total chl *a* biomass and the GPP:CR ratio was significantly high ($r = 0.92$, $n = 13$, $p < 0.0001$) (Fig. 7b), indicating that the GPP:CR ratio increased linearly along with increments in the photosynthetic biomass of the mixed layer. These correlations do not include 3 data points (circled symbols) obtained on 2, 4 and 6 February 2007, when linear relationships were not observed between nitrate and total chl *a* and the GPP:CR ratio (Fig. 7a,b). The possible ecological implications of these 3 data points are discussed later.

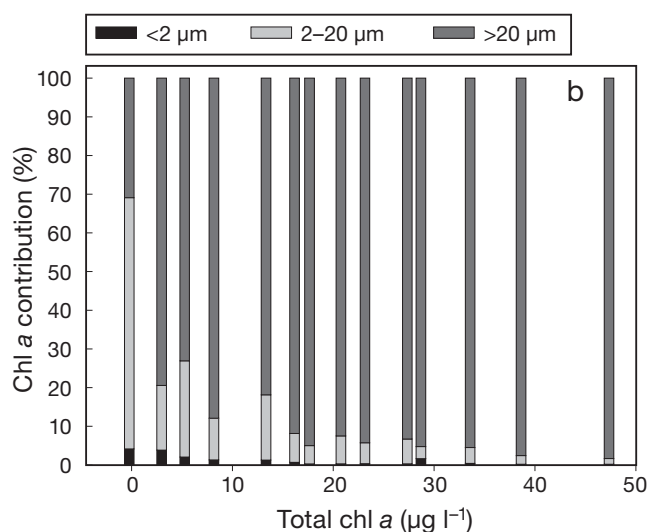
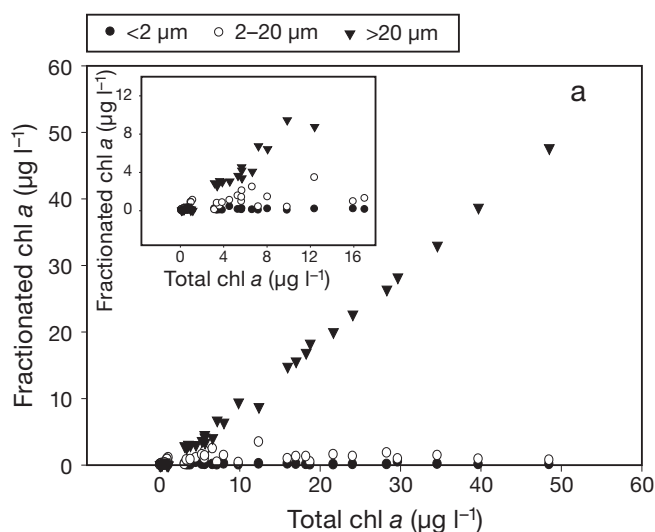


Fig. 6. (a) Relationship between total and fractionated chl *a* (discrete values) in 3 size fractions: microphytoplankton (>20 μm), nanophytoplankton (2 to 20 μm) and picophytoplankton (<2 μm). Inset: the functional relationship between 0 and 16 $\mu\text{g l}^{-1}$ total chl *a*. (b) Relationship between total chl *a* and percentage contribution of size-fractionated chl *a* (discrete values). Data are from Chipana and Mejillones

PNP and GPP

The integrated PNP in the top 20 m of the water column showed high short-term variability in summer and winter, although it was greater in summer (mean = $0.56 \pm 1.5 \text{ g C m}^{-2} \text{ d}^{-1}$, range = 0.076 to $1.27 \text{ g C m}^{-2} \text{ d}^{-1}$) than in winter (mean = $0.13 \pm 0.1 \text{ g C m}^{-2} \text{ d}^{-1}$, range = 0.017 to $0.33 \text{ g C m}^{-2} \text{ d}^{-1}$) (Table 2). The correlation between depth-integrated PNP and GPP was significantly high ($r = 0.71$, $n = 9$, $p < 0.05$) when the system was autotrophic. No association was found between depth-integrated PNP and GPP when the system was net heterotrophic. PNP constituted a substantial fraction of the GPP (mean = 51%, range = 1.7 to 115%) during net heterotrophy but a low percentage during net autotrophy (mean = 5.2%, range = 2 to 12%) (Table 2).

DISCUSSION

Oceanographic variability and biological response

The climatology of northern Chile, based on 30 yr of hydrographic data, shows the presence of a seasonal maximum in alongshore wind stress in late spring and summer (Blanco et al. 2001). The cross-shelf vertical structure of temperature and salinity shows that verti-

Table 2. Summary of integrated gross primary production (GPP), community respiration (CR), net ecosystem metabolism (GPP:CR ratio), prokaryote net production (PNP) and photosynthetic carbon transfer through prokaryotes (PNP/GPP) from the CENSOR cruise in Chipana (21° S) and Mejillones (23° S), northern Chile. nd: no data

Area	Date (dd/mm/yy)	GPP (g C m ⁻² d ⁻¹)	CR (g C m ⁻² d ⁻¹)	GPP:CR ratio	PNP (g C m ⁻² d ⁻¹)	PNP/GPP (%)
Chipana	23/07/05	10.4	3.21	3.24	0.33	3.17
	25/07/05	3.62	1.59	2.28	0.29	8.01
Mejillones	24/01/06	3.64	1.84	1.98	0.076	2.08
	26/01/06	1.54	0.95	1.62	0.104	6.75
	28/01/06	3.75	2.21	1.7	0.168	4.48
Chipana	04/02/06	2.23	4.18	0.53	0.54	24.21
	06/02/06	0.64	1.29	0.5	0.74	115.6
	08/02/06	1.71	2.41	0.71	0.26	15.2
	02/07/06	0.96	1.2	0.8	0.017	1.77
	04/07/06	0.91	0.9	1.01	0.02	2.19
	06/07/06	0.72	0.63	1.14	0.024	3.33
	08/07/06	4.52	2.06	2.19	nd	nd
	02/02/07	0.8	3.58	0.22	0.65	81.25
	04/02/07	2.31	4.36	0.53	0.78	33.76
	06/02/07	1.46	3.18	0.46	1.27	86.98
	08/02/07	8.6	3.08	2.79	1.04	12.09

cal stratification is strongest in summer and weakest in winter (Blanco et al. 2001). In addition, studies of the autotrophic community structure carried out in coastal areas off northern Chile have demonstrated that both phytoplankton abundance and species composition vary seasonally (Herrera & Escribano 2006) and that chl *a* concentrations in the water column are higher in spring (Morales et al. 1996) than in winter (Thiel et al. 2007). Nevertheless, our comparison of summer and winter GPP did not show marked seasonality; rather, high integrated GPP values occurred during periods of maximal intensification of wind-driven upwelling (summer, GPP = 9.3 g C m⁻² d⁻¹; Daneri et al. 2000) as well as periods of low upwelling (winter, GPP = 10.4 g C m⁻² d⁻¹; present study). The lack of seasonality in GPP could be due to the permanent equatorward winds gener-

ated by the South Pacific Anticyclone in northern Chile (Rutllant & Montecino 2002).

In northern Chile, successive upwelling events lead to the dominance of chain-forming diatoms interrupted by the transitory dominance of small flagellated cells during warm conditions (Herrera & Escribano 2006). Changes in the direction and persistence of the upwelling, which is driven by wind stress on a synoptic scale (6 d), appear to be an important factor modulating phytoplankton size structure. For instance, in July 2006, the lowest GPP rates were observed when the wind direction was clearly not favourable to upwelling (i.e. 2, 4 and 6 July). When the wind again became favourable to upwelling (i.e. 8 July 2006), GPP increased almost 5-fold (Table 2) in association with a declining contribution of nanophytoplankton and an increment in the microphytoplankton classes (Table 1). In a simultaneous study, Aguilera et al. (2009) reported short-term variability of the taxonomic composition of the phytoplankton community. These authors showed daily changes (3 to 5 d) in the diversity and richness of nanoplankton and microplankton fractions coupled to an intermittent upwelling regime.

The variability observed in the net ecosystem metabolism (as GPP:CR ratio) of the HCS (e.g. Eissler & Quiñones 1999, Montero et al. 2007) reflects spatial and temporal decoupling between photosynthesis and respiration that is dependent on the physical-biological variability of the ocean. Consequently, respiration and photosynthesis are not in balance on most temporal and spatial scales (e.g. del Giorgio et al. 1998, Duarte & Agustí 1998, Eissler & Quiñones 1999). In the present

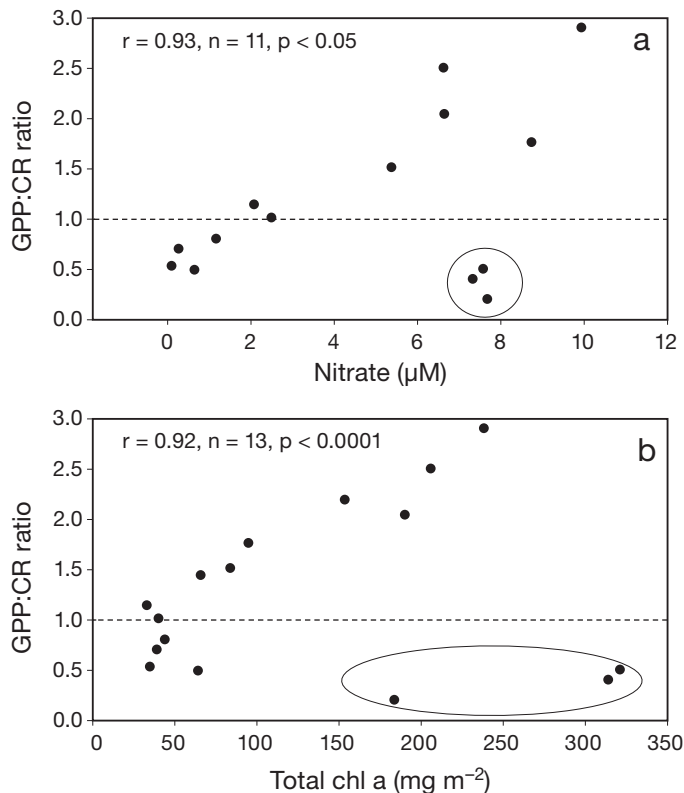


Fig. 7. Relationship between the GPP:CR ratio and (a) mean nitrate concentrations from 0 to 20 m depth and (b) total chl *a* for cruises in Chipana and Mejillones. GPP and CR rates and chl *a* biomass were depth-integrated within the first 20 m of the water column. The correlation analysis does not include the 3 circled outliers obtained on 2, 4 and 6 February 2007.

Horizontal dashed line: GPP:CR = 1

study, we observed that the GPP:CR ratio varied by over one order of magnitude, while the net ecosystem metabolism for the whole data set showed a tendency to be net autotrophic (GPP:CR ratio >1). Short-term variability (6 d) in the GPP:CR ratio was also observed (Table 2); this was likely a response to the variable intensity of upwelling, especially on daily and weekly scales (Escribano et al. 2004a).

On 2, 4 and 6 July 2006, we observed an increase in the relative proportion of pico- (34%) and nanophytoplankton (64%) when the 15°C thermocline and oxycline were deeper and nutrients were low (Table 1, Fig. 4). On these dates, the GPP:CR ratio ~ 1 (range = 0.8 to 1.1) was associated with a non-upwelling period (Fig. 5). A near-equilibrium community ecosystem metabolism (GPP:CR ratio of ~ 1) has also been observed during periods of upwelling relaxation or weak upwelling in the Ria de Vigo (Moncoiffé et al. 2000). On 2, 4, 6 and 8 February 2007, large cells were dominant (>86%), and the water column presented cold, nutrient-rich conditions identified by shallow thermoclines and oxyclines (Fig. 4c). During this period, the GPP:CR ratio varied drastically from net heterotrophic (0.22) to net autotrophic (2.8) (Table 2). These differences (observed in July 2006 vs. February 2007) occurred during the development of the 'weak to moderate' 2006 to 2007 El Niño event (McPhaden 2008). According to McPhaden (2008), the oceanographic perturbations began approximately in June 2006, peaked in November to December 2006 and ended early in February 2007. Therefore, the July 2006 and February 2007 cruises might represent the change from 'abnormal' to 'normal' oceanographic conditions. It is recognized that mesoscale vertical motion directly controls the phytoplankton size structure in the ocean (Rodríguez et al. 2001). In northern Chile, changes in the size-fractionated primary production and biomass have been observed during interannual atmospheric forcing (1997 to 1998 El Niño), as reflected by the dominance of pico- and nanophytoplankton (> 50%) and low primary production rates (González et al. 1998, Iriarte et al. 2000, Iriarte & González 2004). Here, we note that the occurrence of intraseasonal atmospheric forcing characterized by 'weak to moderate anomalies' during the 2006–2007 El Niño (McPhaden 2008) may affect the phytoplankton size structure and, consequently, the balance between primary production and community respiration in the mixed layer.

Relationship between nitrate, chl *a* and the GPP:CR ratio

The functional relationship between average nitrate concentrations and the GPP:CR ratio in the mixed layer

was highly correlated (Fig. 7a), emphasizing the importance of upwelling for decoupling the production and consumption of organic matter toward net autotrophy. Nutrient availability has been shown to regulate the plankton community structure and dynamics, generating temporal and/or spatial decoupling in the GPP:CR ratio (McAndrew et al. 2007, Montero et al. 2007). The 3 circled outliers associated with the lowest GPP:CR ratio (range = 0.2 to 0.5) in Fig. 7a represent a situation in which the percentage of GPP utilized by heterotrophic prokaryotes (PNP/GPP) was extremely high from 2 to 6 February 2007 (range = 34 to 87%) (see Table 2). Considering that heterotrophic prokaryotes consume on average 40 to 50% of the primary production across systems (Cole et al. 1988, Ducklow & Carlson 1992), our results suggest that other sources of dissolved organic matter fueled the metabolic demand of the heterotrophic prokaryotes. Simultaneous studies carried out in Chipana showed that the period from 2 to 6 February 2007 corresponded to a situation in which autotrophic dinoflagellates abundance was 2 orders of magnitude greater ($>1000 \text{ cell ml}^{-1}$) than that of diatoms ($<90 \text{ cell ml}^{-1}$) (Aguilera et al. 2009). There was a strong increase in *Gonyaulax grindleyi* abundance during the first few days of this period (2 to 5 February 2007), whereas an abrupt drop in their abundance was observed between 6 and 9 February 2007 (Aguilera et al. 2009). Dinoflagellates have been characterized as the second most important component of the phytoplankton community after diatoms in the coastal area of northern Chile (Herrera & Escribano 2006). However, this situation can change because of the replacement of diatoms by dinoflagellates species with a competitive advantage, such as the production of toxins or daily vertical migration when the water column becomes stratified. The lowest GPP:CR ratios (<1) were associated with the occurrence of a massive *Gonyaulax* bloom in early February 2007, whereas GPP:CR ratios >1 were observed when the *Gonyaulax* bloom decayed abruptly during late February 2007. Given the previous statements, we did not include these data points (2 to 6 February 2007) in the correlations shown in Fig. 7a,b because we considered that they were not representative of the trends we were observing in this study. Drastic changes in the microphytoplankton species composition and abundance may increase the contribution of phytoplankton respiration to overall community respiration.

We also observed a significant correlation between total chl *a* biomass and the GPP:CR ratio (Fig. 7b). Because the microphytoplankton contribution varies almost linearly with total chl *a* biomass ($r^2 = 0.99$, $p < 0.0001$; Fig. 6a,b), we expected the increase in dominance of large phytoplankton (in terms of contribution and biomass) to generate greater net autotrophy. The-

oretical models suggest a tight linkage between phytoplankton size structure, food web pathways and the fate of biogenic carbon within the microbial plankton community (Legendre & Le Fèvre 1989, Tremblay & Legendre 1994, Legendre & Michaud 1998). Basically, these studies indicate that the heightened dominance of large phytoplankton cells increases the carbon export. Our results suggest that the greater contribution of large phytoplankton cells reflects an autotrophic response of the net ecosystem metabolism to higher nitrate concentrations in the mixed layer. However, we also observed that these relationships may not occur because changes in the dominance of microphytoplankton species may impact the carbon fluxes (through the planktonic food web) and, therefore, the balance between primary production and CR.

Relationship between GPP and prokaryote net production

High correlations between GPP and PNP were found during periods when the system was net autotrophic. Given that the extracellular release of dissolved organic matter (DOM) is linearly related to primary production across diverse aquatic systems (Baines & Pace 1991), we expect that PNP was responding to an extracellular release of DOM during active photosynthesis by phytoplankton. In contrast, when the system was net heterotrophic, PNP was not correlated with GPP, which probably indicates that prokaryotes were growing in response to a greater diversity of dissolved molecules produced by mechanisms quite different from algal extracellular release. Said mechanisms include, for instance, the egestion of unassimilated prey material by protozoan grazers (20–30%) and metazoan zooplankton (10–20%), and viral infections of host cells (Nagata 2000 and references therein). Our results showed that PNP constituted, on average, up to 50% of the GPP when the system was dominated by heterotrophic processes, whereas <14% was channelled by heterotrophic prokaryotes when the system was dominated by autotrophic processes (Table 2). The evidence from the literature indicates that the release of DOM by grazers is greater than that of phytoplankton (Nagata 2000). Moreover, empirical evidence indicates that the average extracellular release by phytoplankton (13%) is not sufficient to fulfill the bacterial carbon demand (Nagata 2000). Thus, over 66% of the heterotrophic prokaryote demand must be supplied by DOM sources other than direct release by phytoplankton (Nagata 2000). Herein, we have demonstrated that the degree of coupling of heterotrophic prokaryote production and GPP varies with changes in the dominance of autotrophic and heterotrophic processes in the

microplanktonic community. In addition, we suggest that the amount of organic matter processed by heterotrophic prokaryotes is greater when the organic matter consumption processes dominate the carbon fluxes in the microplanktonic community.

Concluding remarks

The microbial community inhabiting the mixed layer of the coastal zone off northern Chile is subjected to marked trophic gradients triggered by synoptic-scale shifts in the upwelling driven by wind stress. Drastic changes in the wind-stress direction and hydrographical and chemical characteristics of the mixed layer influenced the phytoplankton size structure, primary production rates and net ecosystem metabolism during the development of the 'weak' 2006 to 2007 El Niño event in northern Chile.

We found that an increase in the biomass of large phytoplankton cells generates net autotrophy in response to the increase of nitrate concentrations in the mixed layer, emphasizing that the degree of decoupling between GPP and CR may be primarily controlled by upwelling in this region. Our experiments showed that the degree of coupling between heterotrophic prokaryote production and GPP, as well as the amount of organic matter processed by heterotrophic prokaryotes, varies with changes in the dominance of autotrophic and heterotrophic processes in the microplankton community.

Acknowledgements. We thank P. Hidalgo, M. Fuentes, P. Mendoza, K. Donoso, C. Perez, E. Isla, P. Homs and I. Montes for their valuable contribution during field work, laboratory analyses and data processing. B.J. was supported by a doctoral fellowship of the CENSOR project (Climate variability and El Niño Southern Oscillation, awarded to Dr. R. Escobedo) and was funded by the EUC and the PCBT of Chile, RUE-O2; the latter also supported a research visit to Europe for 4 months. B.J. and G.D. were also supported by the Universidad del Mar and CIEP. R.A.Q. was funded by the COPAS Center (CONICYT, Chile). We acknowledge the help of the captain and crew of the RVs 'El Rigel's' and 'Purihalar' (Universidad Arturo Prat, Chile).

LITERATURE CITED

- Aguilera V, Escobedo R, Herrera L (2009) High frequency responses of nanoplankton and microplankton to wind-driven upwelling off northern Chile. *J Mar Syst* 78:124–135
- Azam F, Fenchel T, Field JG, Gray JS, Meyer-Reil LA, Thingstad F (1983) The ecological role of water-column microbes in the sea. *Mar Ecol Prog Ser* 10:257–263
- Baines SB, Pace ML (1991) The production of dissolved organic matter by phytoplankton and its importance to bacteria: patterns across marine and freshwater systems. *Limnol Oceanogr* 36:1078–1090

- Barber RT, Sanderson M, Lindley ST, Chai F and others (1996) Primary productivity and its regulation in the equatorial Pacific during and following the 1991–1992 El Niño. *Deep-Sea Res II* 43:933–969
- Blanco JL, Thomas AC, Carr ME, Strub PT (2001) Seasonal climatology of hydrographic conditions in the upwelling region off northern Chile. *J Geophys Res* 106:11451–11467
- Böttjer D, Morales CE (2005) Microzooplankton grazing in a coastal embayment off Concepción, Chile (~36°S) during non-upwelling conditions. *J Plankton Res* 27:383–391
- Cole JJ, Findlay S, Pace ML (1988) Bacterial production in fresh and saltwater ecosystems: a cross-system overview. *Mar Ecol Prog Ser* 43:1–10
- Cuevas A, Daneri G, Jacob B, Montero P (2004) Microbial abundance and activity in the seasonal upwelling area off Concepción (~36°S), central Chile: a comparison of upwelling and non-upwelling conditions. *Deep-Sea Res II* 51:2427–2440
- Daneri G, Dellarossa V, Quiñones R, Jacob B, Montero P, Ulloa O (2000) Primary production and community respiration in the Humboldt Current System off Chile and associated oceanic areas. *Mar Ecol Prog Ser* 197:41–49
- del Giorgio PA, Cole JJ, Cimleris A (1998) Respiration rates in bacteria exceed phytoplankton production in unproductive aquatic systems. *Nature* 385:148–151
- Duarte CM, Agustí S (1998) The CO₂ balance of unproductive aquatic ecosystems. *Science* 281:234–236
- Ducklow HW, Carlson CA (1992) Oceanic bacterial production. *Adv Microb Ecol* 12:113–181
- Eissler Y, Quiñones RA (1999) Microplanktonic respiration off northern Chile during El Niño 1997–1998. *J Plankton Res* 21:2263–2283
- Escribano R, Rosales S, Blanco JL (2004a) Understanding upwelling circulation of Bahía Antofagasta (northern Chile): a numerical modelling approach. *Cont Shelf Res* 24:37–53
- Escribano R, Daneri D, Farías L, Gallardo VA and others (2004b) Biological and chemical consequences of the 1997–98 El Niño in the Chilean coastal upwelling system: a synthesis. *Deep-Sea Res II* 51:2389–2411
- González HE, Daneri G, Figueroa D, Iriarte JL and others (1998) Producción primaria y su destino en la trama trófica pelágica y océano profundo e intercambio océano-atmósfera de CO₂ en la zona norte de la Corriente de Humboldt (23°S): posibles efectos del evento El Niño, 1997–98 en Chile. *Rev Chil Hist Nat* 71:429–458
- Herndl GJ, Reinthaler T, Teira E, van Aken H, Veth C, Pernthaler J (2005) Contribution of Archaea to total prokaryotic production in the deep Atlantic Ocean. *Appl Environ Microbiol* 71:2303–2309
- Herrera L, Escribano R (2006) Factors structuring the phytoplankton community in the upwelling site off El Loa River in northern Chile. *J Mar Syst* 61:13–38
- Iriarte JL, González HE (2004) Phytoplankton size structure during and after the 1997/98 El Niño in a coastal upwelling area of the northern Humboldt Current System. *Mar Ecol Prog Ser* 269:83–90
- Iriarte JL, Pizarro G, Troncoso VA, Sobarzo M (2000) Primary production and biomass size-fractionated phytoplankton off Antofagasta, Chile (23–24°S) during pre-El Niño and El Niño 1997. *J Mar Syst* 26:37–51
- Jahnke RA, Craven DB (1995) Quantifying the role of heterotrophic bacteria in the carbon cycle: a need for respiration rate measurements. *Limnol Oceanogr* 40:436–441
- Karner MB, Delong EF, Karl DM (2001) Archaeal dominance in the mesopelagic zone of the Pacific Ocean. *Nature* 409:507–510
- Kemp WM, Smith EM, Marvin-DiPasquale M, Boynton WR (1997) Organic carbon balance and net ecosystem metabolism in Chesapeake Bay. *Mar Ecol Prog Ser* 150:229–248
- Kjørboe T (1996) Material flux in the water column. In: Jørgensen BB, Richardson K (eds) *Eutrophication in coastal ecosystems*. Coastal and estuarine studies 52. American Geophysical Union, Washington, DC, p 67–94
- Laws EA (1991) Photosynthetic quotients, new production and net community production in the open ocean. *Deep-Sea Res A* 38:143–167
- Leal CP, Quiñones RA, Chávez C (2010) What factors affect the decision making process when setting TACs? The case of Chilean fisheries. *Mar Policy* 34:1183–1195
- Legendre L, Le Fèvre J (1989) Hydrodynamical singularities as controls of recycled versus export production in oceans. In: Berger WH, Smetacek VS, Wefer G (eds) *Productivity of the ocean: present and past*. Wiley, London, p 49–63
- Legendre L, Michaud J (1998) Flux of biogenic carbon in oceans: size-dependent regulation by pelagic food webs. *Mar Ecol Prog Ser* 164:1–11
- Legendre L, Rassoulzadegan F (1995) Plankton and nutrient dynamics in marine waters. *Ophelia* 41:153–172
- Legendre L, Gosselin M, Hirche HJ, Kattner G, Rosenberg G (1993) Environmental control and potential fate of size-fractionated phytoplankton production in the Greenland Sea (75°N). *Mar Ecol Prog Ser* 98:297–313
- McAndrew PM, Björkman KM, Church MJ, Morris PJ, Jachowski N, Williams PJ le B, Karl DM (2007) Metabolic response of oligotrophic plankton communities to deep water nutrient enrichment. *Mar Ecol Prog Ser* 332:63–75
- McPhaden MJ (2008) Evolution of the 2006–2007 El Niño: the role of intraseasonal to interannual time scale dynamics. *Adv Geosci* 14:219–230
- Moncoiffé G, Alvarez-Salgado XA, Figueiras FG, Savidge G (2000) Seasonal and short-time-scale dynamics of microplankton community production and respiration in an inshore upwelling system. *Mar Ecol Prog Ser* 196:111–126
- Montecino V, Strub TP, Chavez F, Thomas A, Tarazona J, Baumgartner T (2006) Bio-physical interactions off western south-America. In: Robinson AR, Brink K (eds) *The global coastal ocean*. Interdisciplinary regional studies and syntheses. Harvard University Press, Cambridge, MA, p 329–390
- Montero P, Daneri G, Cuevas LA, González HE, Jacob B, Lizárraga L, Menchel E (2007) Productivity cycles in the coastal upwelling area off Concepción: the importance of diatoms and bacterioplankton in the organic carbon flux. In: Escribano R, Schneider W (eds) *The structure and functioning of the coastal upwelling in central/southern Chile*. *Prog Oceanogr* 75:518–530
- Morales CE, Blanco JL, Braun M, Reyes H, Silva N (1996) Chlorophyll-*a* distribution and associated oceanographic conditions in the upwelling off northern Chile during the winter and spring 1993. *Deep-Sea Res I* 43:267–289
- Nagata T (2000) Production mechanisms of dissolved organic matter. In: Kirchman DL (ed) *Microbial ecology of the oceans*. Wiley & Sons, New York, NY, p 121–152
- Nielsen TG, Hansen B (1995) Plankton community structure and carbon cycling on the western coast of Greenland during and after the sedimentation of a diatom bloom. *Mar Ecol Prog Ser* 125:239–257
- Nixon SW, Pilson MEQ (1984) Estuarine total system metabolism and organic exchange calculated from nutrient ratios: an example from Narragansett Bay. In: Kennedy VS (ed) *The estuary as a filter*. Academic Press, Orlando, FL, p 261–290

- Pomeroy LR (1974) The ocean's food web: a changing paradigm. *Bioscience* 24:499–504
- Quiñones RA, Platt T (1991) The relationships between the f-ratio and the P:R ratio in the pelagic ecosystem. *Limnol Oceanogr* 36:211–213
- Quiñones RA, Levipan H, Urrutia H (2009) Spatial and temporal variability of planktonic archaeal abundance in the Humboldt Current System off Chile. *Deep-Sea Res II* 56:1073–1082
- Quiñones RA, Gutiérrez MH, Daneri G, Gutiérrez DA, González HE, Chávez F (2010) Pelagic carbon fluxes in the Humboldt Current System. In: Liu KK, Atkinson L, Quiñones RA, Talaue-McManus L (eds) Carbon and nutrient fluxes in global continental margins: a global synthesis. Springer-Verlag, New York, NY, p 44–64
- Robinson (2008) Heterotrophic bacterial respiration. In: Kirchman DL (ed) *Microbial ecology of the oceans*, 2nd edn, Vol. 9. Wiley & Sons, New York, NY, p 299–334
- Rodríguez J, Tintoré J, Allen JT, Blanco JM and others (2001) Mesoscale vertical motion and the size structure of phytoplankton in the ocean. *Nature* 410:360–363
- Rutllant J, Montecino V (2002) Multiscale upwelling forcing cycles and biological response off north central Chile. *Rev Chil Hist Nat* 75:217–231
- Sieburth JMcN, Smetacek V, Lenz J (1978) Pelagic ecosystem structure: Heterotrophic compartments of plankton and their relationship to plankton size fractions. *Limnol Oceanogr* 33:1225–1227
- Simon M, Azam F (1989) Protein content and protein synthesis rates of planktonic marine bacteria. *Mar Ecol Prog Ser* 51:201–213
- Smith SV, Hollibaugh JT (1997) Annual cycle and interannual variability of ecosystem metabolism in a temperate climate embayment. *Ecol Monogr* 67:509–533
- Smith EM, Kemp WM (2001) Size structure and the production/respiration balance in a coastal plankton community. *Limnol Oceanogr* 46:473–485
- Steele JH (1974) *The structure of marine ecosystems*. Harvard University Press, Cambridge, MA
- Strickland JDH (1960) Measuring the production of marine phytoplankton. *Bull Fish Res Board Can* 122:1–72
- Strickland JD, Parsons TR (1968) *A practical handbook of seawater analysis*. Bull Fish Res Board Can 167:71–75
- Tamigneaux E, Legendre L, Klein B, Mingelbier M (1999) Seasonal dynamics and potential fate of size-fractionated phytoplankton in a temperate nearshore environment (western Gulf of St. Lawrence, Canada). *Estuar Coast Shelf Sci* 48:253–269
- Teira E, Serret P, Fernández E (2001) Phytoplankton size-structure, particulate and dissolved organic carbon production and oxygen fluxes through microbial communities in the NW Iberian coastal transition zone. *Mar Ecol Prog Ser* 219:65–83
- Thiel M, Macaya EC, Acuna E, Arntz WE and others (2007) The Humboldt current system of northern and central Chile. Oceanographic processes, ecological interactions and socioeconomic feedback. *Oceanogr Mar Biol Annu Rev* 45:195–344
- Tremblay JÉ, Legendre L (1994) A model for the size-fractionated biomass and production of marine phytoplankton. *Limnol Oceanogr* 39:2004–2014
- Troncoso VA, Daneri G, Cuevas LA, Jacob B, Montero P (2003) Bacterial carbon flow in the Humboldt Current System off Chile. *Mar Ecol Prog Ser* 250:1–12
- Ulloa O, Pantoja S (2009) The oxygen minimum zone of the eastern South Pacific. *Deep-Sea Res II* 56:987–991
- Vargas CA, Martínez R, Cuevas LA, Pavez MA and others (2007) Interplay between microbial and classical food webs in a highly productive coastal upwelling area. *Limnol Oceanogr* 52:1495–1510
- Williams PJ le B (1981) Incorporation of microheterotrophic processes into the classical paradigm of the planktonic food web. *Kiel Meeresforsch Sonderh* 5:1–28

Editorial responsibility: Graham Savidge, Portaferry, UK

*Submitted: October 14, 2009; Accepted: February 3, 2011
Proofs received from author(s): May 10, 2011*